RESEARCH ARTICLE

Key Points:
- Observations of Reynolds stresses were used to infer locally relevant pressure gradients
- Inter-annual differences in circulation were not due local along-shelf pressure gradients
- Local pressure gradients can alter the exchange between the Gulf of Maine and Mid-Atlantic Bight

Correspondence to:
A. R. Kirincich,
akirincich@whoi.edu

Drivers of spring and summer variability in the coastal ocean offshore of Cape Cod, MA

Anthony R. Kirincich[1] and Glen G. Gawarkiewicz[1]

[1]Department of Physical Oceanography, Woods Hole Oceanographic Institution, Woods Hole, Massachusetts, USA

Abstract The drivers of spring and summer variability within the coastal ocean east of Cape Cod, Massachusetts, a critical link between the Gulf of Maine and Mid-Atlantic Bight, are investigated using 2 years of shipboard and moored hydrographic and velocity observations from 2010 and 2011. The observations reveal sharp differences in the spring transition and along-shelf circulation due to variable freshwater and meteorological forcing, along with along-shelf pressure gradients. The role of the along-shelf pressure gradient is inferred using in situ observations of turbulent momentum flux, or Reynolds stresses, estimated from the ADCP-based velocities using recently developed methods and an inversion of the along-shelf momentum balance. During spring, the locally relevant along-shelf pressure gradient contains a sizable component that is not coupled to the along-shelf winds and often opposes the regional sea level gradient. Together with the winds, local pressure gradients dominate along-shelf transport variability during spring, while density-driven geostrophic flows appear to match the contribution of the local winds during summer. These results suggest that local effects along the Outer Cape have the potential to cause significant changes in exchange between the basins.

1. Introduction

The coastal current present along the eastern shore of Cape Cod, Massachusetts is an important choke point for the circulation leaving the Gulf of Maine (GOM, Figure 1). Flows along this narrow shelf, referred to here as the Outer Cape Coastal Current (OCCC), essentially drain the Gulf, connecting the waters formed in the northern and central parts of the GOM to Georges Bank and the Mid-Atlantic Bight (MAB) to the south [*Pettigrew et al.*, 2005]. Thus, the dynamics of the coastal current, its drivers, and sources of variability, can have a larger than expected regional impact; controlling retention in the GOM, setting the inflow hydrographic conditions for the MAB, restricting the transport of harmful algal blooms (HABs) from source regions in the GOM southward, and serving as a barrier for the northward exchange or transport of pelagic marine organisms [*Pringle et al.*, 2011; *He et al.*, 2008; *McGillicuddy et al.*, 2003].

This study investigates the dynamics and variability present in the OCCC during the spring transition using the results of a 2 year observational effort to determine the relative influences of local versus regional dynamics in controlling the circulation and the transport between the basins. Understanding the variability of this communication between the Gulf of Maine and areas to the south is an important part of our efforts to understand coastal circulation along the eastern United States and its effects on marine ecosystems. In addition to responding to basin-wide forcings and regional freshwater runoff, local winds and flow-topography effects should contribute to variability along the Outer Cape and control the along-shelf transport of water masses in the area. Thus, this study focuses on the OCCC during the key transitional period between the weakly stratified conditions present at the end of winter, and the more stratified summer-time conditions to document the effects of local and nonlocal oceanographic processes on the dynamics present as the water column begins to stratify. The observational effort, carried out in the spring of 2010 and the spring and summer of 2011 utilized across-shelf hydrographic surveys and the deployment of a series of moorings designed to provide estimates of water column hydrography and velocity as well as enable estimates of turbulent Reynolds stresses.

The vertical divergences of the horizontal Reynolds stresses are a critical component of the dynamics present in coastal flows as they act to redistribute the input or removal of momentum by boundary forces throughout the water column. Recent efforts have documented how ADCP-based velocity observations can
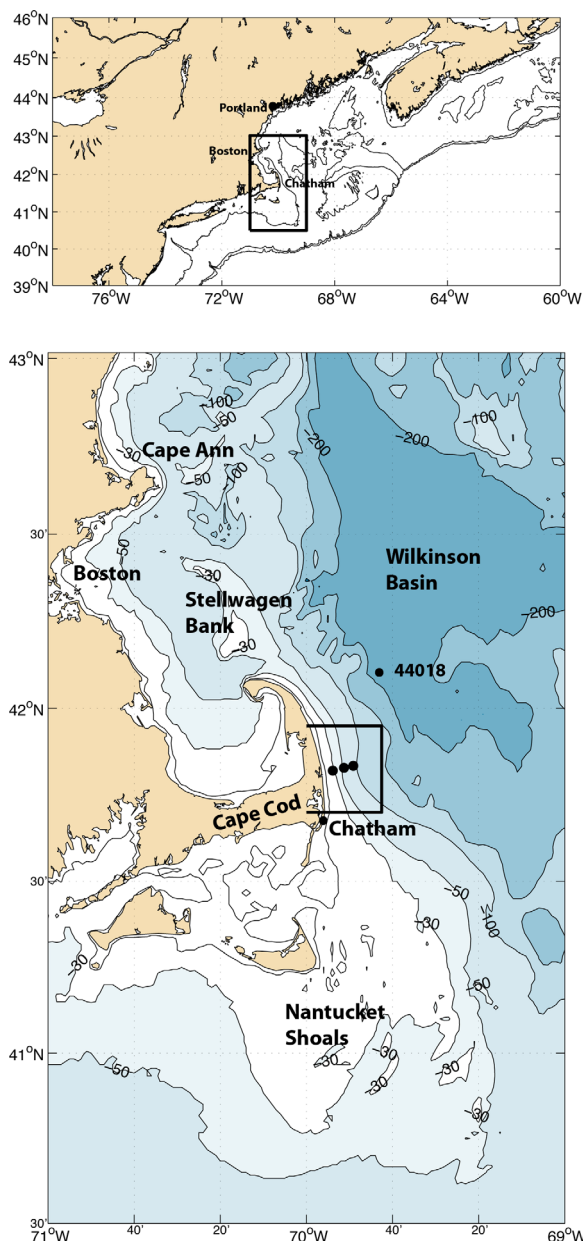
Figure 1. (top) The northeast coastal region of North America from Delaware Bay to Cape Breton with the study area––the southwestern Gulf of Maine––outlined in black. (bottom) The study area within the continental shelf east of the Cape Cod, Massachusetts, the locations of the 30, 60, and 90 m moorings (black dots), the nearby NOAA meteorological buoy (#44018) and locations of various bathymetric and coastal features described in the text.

be used to estimate the horizontal Reynolds stresses [*Stacey et al.*, 1999a, 1999b; *Rosman et al.*, 2008; *Kirincich et al.*, 2010; *Kirincich and Rosman*, 2010]. Previous studies of coastal dynamics have examined the frictional components of circulation via the depth-integrated momentum balances [e.g., *Allen*, 1980; *Lentz et al.*, 1999], where the effects of this momentum transfer is accounted for by the difference between the surface and bottom stresses using drag laws. Direct observations of the Reynolds stresses can more accurately constrain the typical parameterizations of the boundary stresses, offer a more precise understanding of the frictional momentum balances present, and be used to estimate the locally relevant along-shelf pressure gradient [*Kirincich*, 2013].

The paper is organized as follows: a review of previous studies of the Outer Cape Coastal Current (OCCC) and its general characteristics is presented first, followed by details on the shipboard, moored, ancillary observations, and processing methods utilized. Results illustrating the hydrographic and velocity structures present during the 2010 and 2011 spring transitions are then given, followed by an exploration of the along-shelf pressure gradient and the relative contributions of wind, pressure gradients, and across-shelf density gradients to the observed along-shelf velocity. Finally, the relevance of the results to climatological conditions and inter-annual variability are discussed as well as the importance of flow reversals.

2. Previous Efforts on the OCCC

Long the focus of observational efforts [e.g., *Bigelow*, 1927], previous research on the Gulf of Maine has examined the hydrographic and current structure of the western part of the gulf, from Maine to Cape Ann [*Fong et al.*, 1997; *Pettigrew et al.*, 2005; *Churchill et al.*, 2005], within the Massachusetts Bay/ Stellwagen Bank region [*Bothner and Butman*, 2007], and in areas to the south of Cape Cod including Georges Bank [*Chen et al.*, 1995a, 1995b; *Beardsley et al.*, 2003]. In general, the coastal current system in the western Gulf of Maine flows southward along the coast of Maine toward Cape Ann and, in spring and summer, acquires freshwater from the numerous coastal rivers that drain southern Maine and New Hampshire (Figure 2). Entering the coastal waters of Massachusetts, the current bifurcates near Cape Ann, with one branch jumping across a series of bathymetric gaps and ridges to Stellwagen Bank, and a second hugging the coast to flow around Massachusetts Bay. The two potentially merge again at the northern tip of Cape Cod, and flow southward along the narrow shelf east of Cape Cod. To the south of the cape, upon
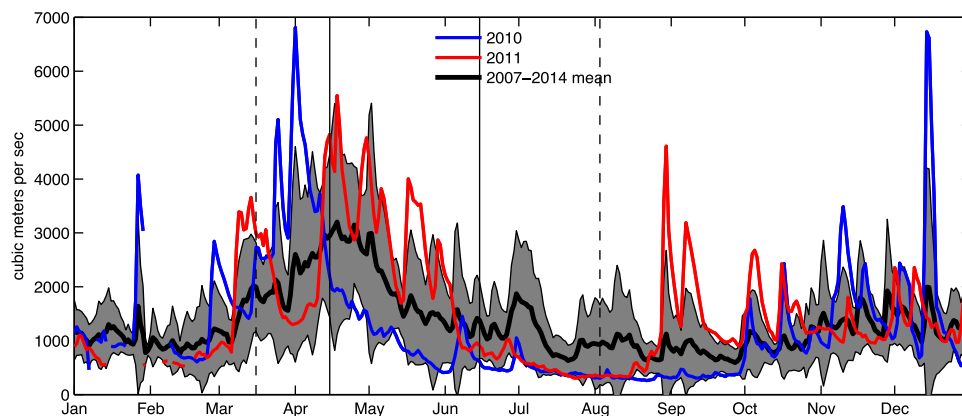
Figure 2. Daily combined discharge estimates from the five major rivers entering the western Gulf of Maine (the Penobscot, Kennebec, Androscoggin, Saco, and Merrimack), based on daily averages from USGS gauging stations (numbers 01034500, 01049265, 01059000, 01066000, and 01100000). (black, grey) The mean and standard deviation of discharge during 2007–2014, and standard deviation window is shown along with estimates for (blue) 2010 and (red) 2011. Solid (dashed) vertical lines denote the spring 2010 (2011) study period.

reaching the Great South Channel, the current bifurcates again, flowing toward Georges Bank to the east or the Mid-Atlantic Bight to the west.

As the transport along the Outer Cape links the water masses of the Gulf of Maine, Georges Bank, and the southern New England shelf, variability of the dynamics present here have implications for biological communities in the region, particularly during the spring and summer seasons. Waters within the OCCC can be quite productive [*Durbin et al.*, 1995]. Work by *Chen et al.* [1995a, 1995b] and *Durbin et al.* [1995] found sharp hydrographic features along the shelf in spring and early summer with significant hydrographic and nutrient variability. The transport of Harmful Algal Blooms (HABs) between the Gulf of Maine and coastal areas to the south contributes to blooms in Nantucket Sound, Georges Bank, and the Middle Atlantic Bight, both onshore and offshore [*McGillicuddy et al.*, 2014; *He et al.*, 2005, 2008; *Anderson et al.*, 2014]. More recent efforts to understand the connectivity of invertebrate larvae along the eastern seaboard of the U.S. have identified the area of the OCCC as an important barrier for larval transport both to the south and north [*Pringle et al.*, 2011].

Despite the significance of the OCCC, our understanding of water mass modification along the Outer Cape, the sources of variability, as well as the relative importance of regional versus local forcings remains limited. It is known that the types of dynamics present over the shelf can play a significant role in determining the fate of water masses transiting the area, setting both the outflow conditions of the Gulf of Maine and the inflow conditions to the Mid-Atlantic Bight [*Brown*, 1998; *Brink et al.*, 2003; *Churchill et al.*, 2005; *Manning et al.*, 2009; *Li et al.*, 2014]. This is particularly true during the transition from winter to summer conditions, where Outer Cape waters change from conditions associated with dense water formation over the midshelf [*Shcherbina and Gawarkiewicz*, 2008a, 2008b] to buoyant plume conditions to temperature-stratified conditions. During this transition, the remnants of wintertime dense water, increased freshwater input and insolation, along with the multiple pathways of circulation around Stellwagen Bank have the potential to lead to variable across-shelf structure of the southward flowing current along the along the Outer Cape. The issue of freshwater transport is particularly complex because inter-annual transports may relate more closely to distant sources rather than river outflows from the western Gulf of Maine [*Shcherbina and Gawarkiewicz*, 2008a]. The across-shelf structure of these varying water masses might predispose the current toward different coastal dynamics depending on the wind or pressure gradients present, resulting in highly variable water mass properties as well as the across-shelf distribution of the along-shelf transport after transiting through the region.

In general, a background along-shelf pressure gradient exists along the Northeastern part of the continental U.S., due to buoyancy input far upstream in the Laborador Sea or Arctic [*Lentz*, 2008, and references therein]. Additional gradients in sea level pressure along the Outer Cape might be the result of coupled responses to basin-scale winds [*Brown*, 1998; *Brown and Irish*, 1992], the local input of freshwater [*Geyer et al.*, 2004], or flow-topography effects. However, how much each contributes to the localized expression
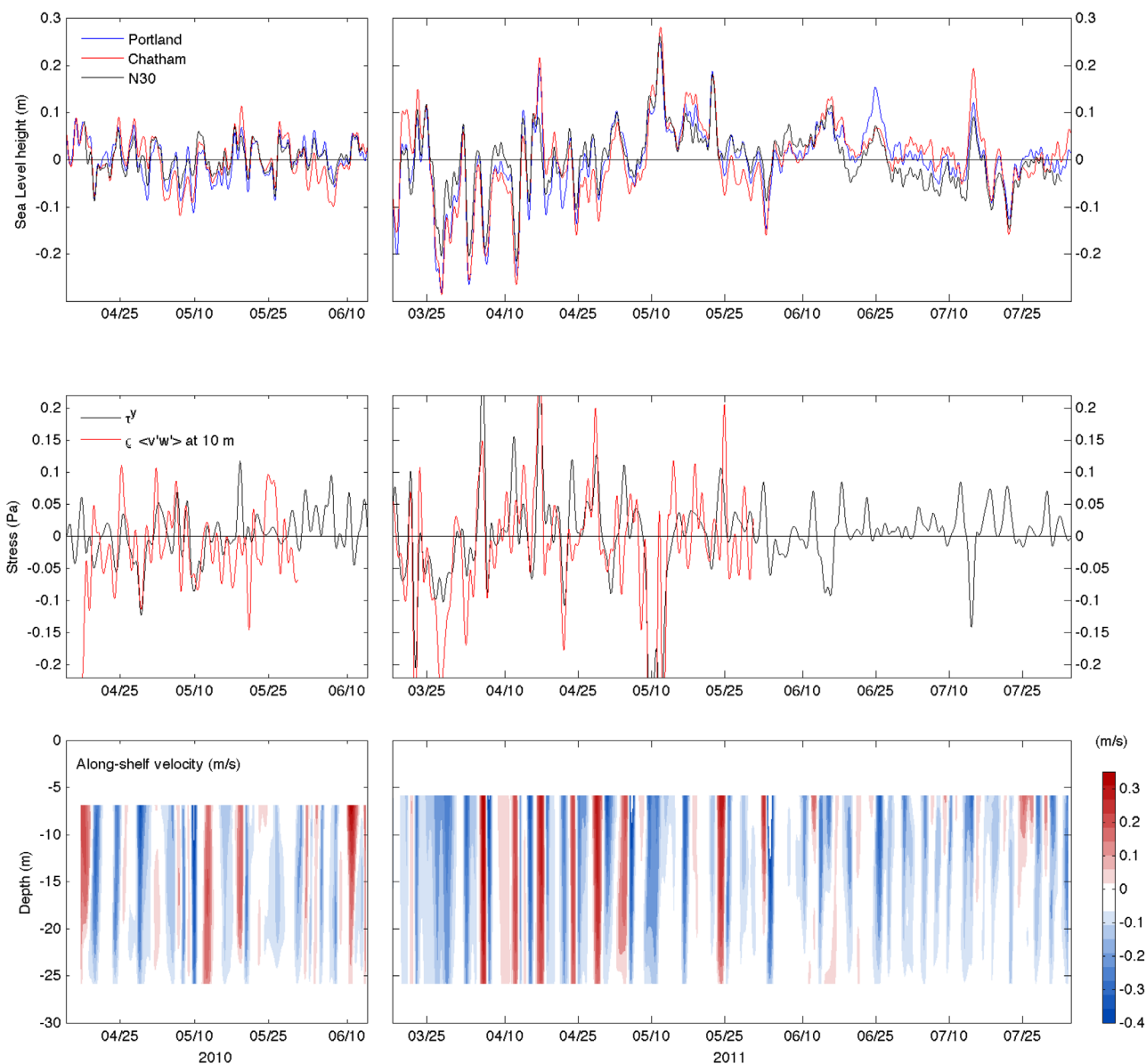
Figure 3. For (left) 2010 and (right) 2011, (top row) the adjusted Sea level height estimates are shown for the (blue) Portland and (red) Chatham stations operated by NOAA, compared to the observed pressure anomalies at the location of (black) N30, the 30 m ADCP bottom lander. (middle row) The along-shelf wind stress, as measured 40 km northeast of the mooring location and the estimated along-shelf vertical Reynolds' stress at 10 m depth. (bottom row) The along-shelf velocity measured by the 30 m ADCP during the spring 2010 and spring 2011 deployments.

of the along-shelf pressure gradient is not known, despite the area's importance as the link between the Gulf of Maine and Mid-Atlantic Bight.

Finally, the Gulf of Maine and Mid-Atlantic Bight have been undergoing significant inter-annual variability in recent years. Examining the variations of the Gulf of Maine coastal current between 2002 and 2011, *Li et al.* [2014] found that the coastal current system was notably weak in 2010, due in part to the advection of warm slope water into the interior of the Gulf of Maine. The slope water intrusion acted to raise the dynamic height of the central basin, weakening the gradient of dynamic height between the interior of the gulf and the coast. This reduced gradient led to the lowest geostrophic velocities observed within the coastal current during the 10 years of analysis. Over longer time scales, *Balch et al.* [2012] have shown that there is a freshening trend in the Western Maine Coastal Current since 1998; related in part to increased river input into the Gulf of Maine basin.
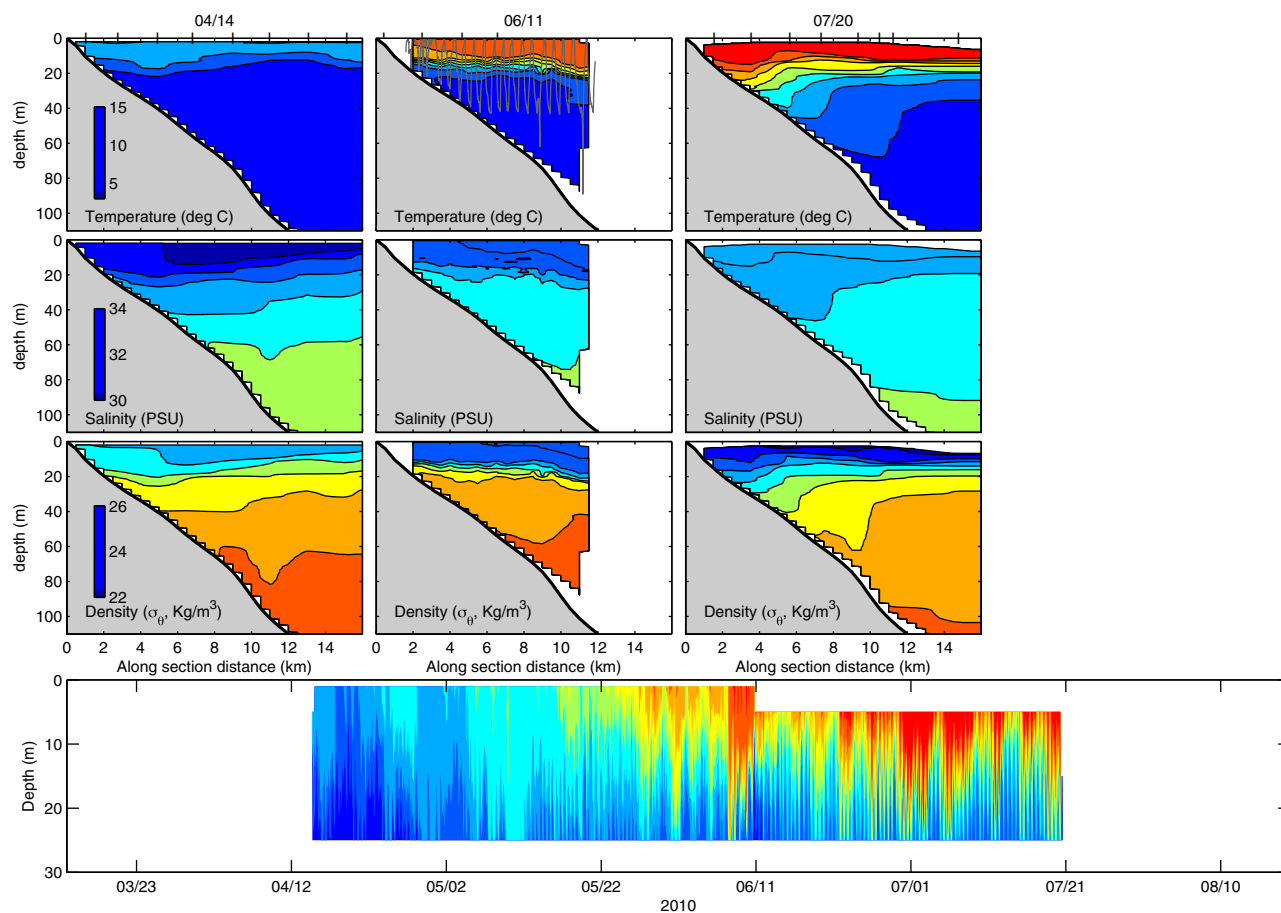
Figure 4. (top) Across-shelf sections of temperature, salinity, and density structure from 14 April, 11 June, and 20 July 2010 along the transect line made using the R/V Tioga's shipboard CTD or a Minibat towed profiler (11 June). (bottom) Water column temperatures at the 30 m mooring location during 2010 using the same color bar as shown for temperature in the top left plot. The Minibat track line or CTD station locations are shown on the top plots.

3. Observations and Data Preparation

During 2010 and 2011, a campaign of hydrographic surveys and moored observations was conducted to measure the seasonal evolution of the OCCC. Seven across-shelf transects of the current were occupied from February to November in 2010 and 4 transects from March to August of 2011 via shipboard CTD casts and towed body or REMUS-AUV based profiling. These transects usually spanned the shelf offshore of Cape Cod, MA (Figure 1) from water depths of 15 m to 120 m, or 0.5 km to 15 km offshore. To augment the sparse temporal observations of the across-shelf hydrography, three deployments of a series of hydrographic and velocity moorings were made for 2 months each in the spring (April–June) and fall (September–November) of 2010 and 4.5 months in the spring and summer (March–August) of 2011. The moorings, located at water depths of 30, 60, and 90 m (Figure 1) or 3.3, 7, and 10 km offshore, made observations of temperature using Onset WaterTemp Pro loggers at 5 m vertical spacing and conductivity-temperature using Seabird SBE 37s at the surface and bottom. A bottom lander, deployed adjacent to the 30 m mooring, observed velocity profiles using a T-RDI Workhorse Sentinel 600 kHz ADCPs and vertical bin sizes of 1 m.

Using the available data, this study focuses on the spring transition during both 2010 and 2011. The temperature and CT sensors, sampled at 5 or 15 min, were averaged to hourly time series. ADCP-based along-beam velocities were sampled at high-frequency––0.5-Hz-ping-rates for 20 min every half hour––to enable estimation of Reynolds stresses as described in Appendix A. From these data, estimates of the vertical structure of the horizontal velocities and Reynolds stresses for water depths of 6 to 28 m, due to the limitations of side-lobe interference for the same hourly time step used for the hydrographic samples. The velocity and stress results were rotated into an across and along-shelf coordinate system defined by the principal axis of the depth-averaged, subtidal velocity. This axis was approximately along-shelf in direction, having a
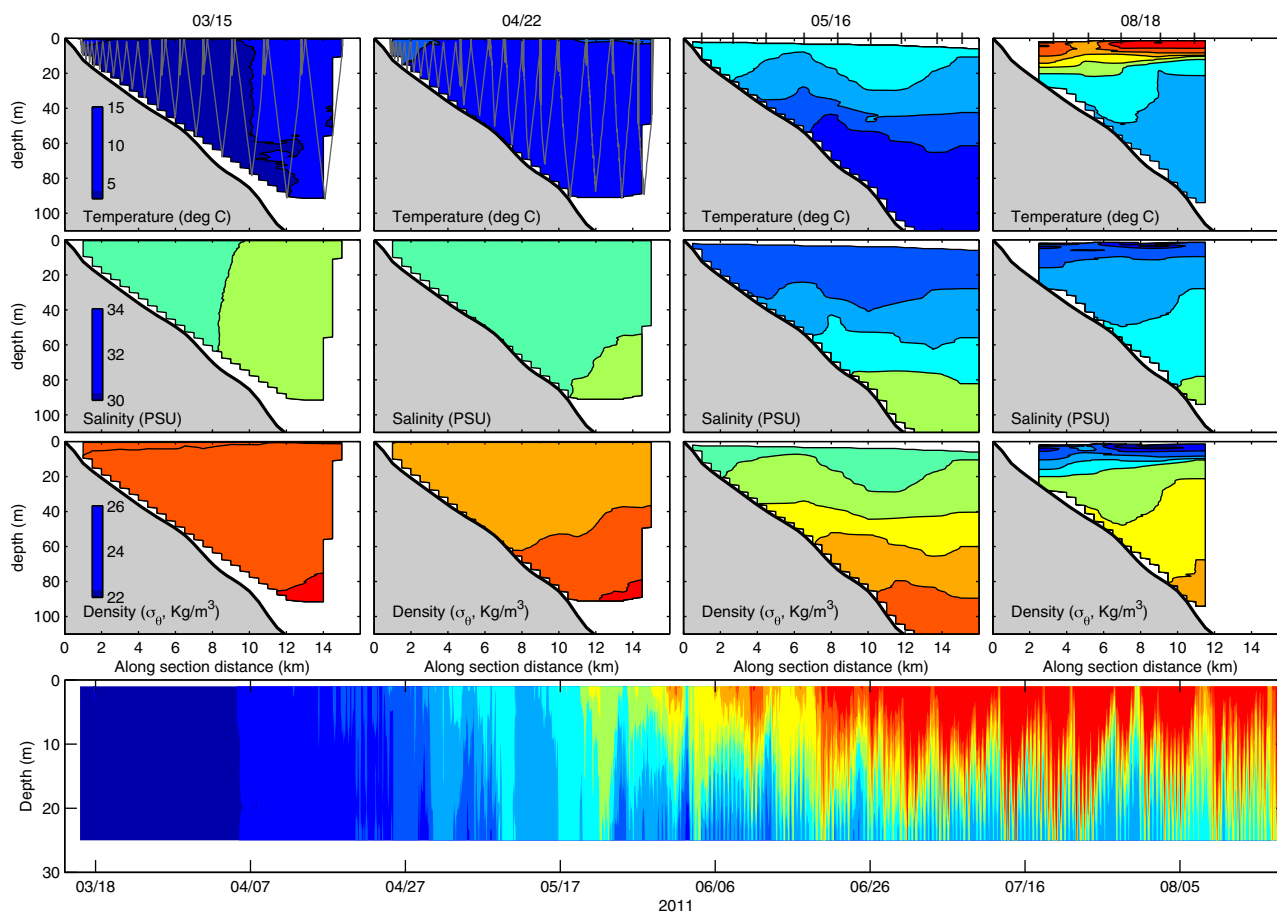
Figure 5. Similar to Figure 4 but for 2011. (top) Across-shelf sections of temperature, salinity, and density structure from 15 March, 22 April, 16 May, and 18 August 2011 along the transect line made using a REMUS-AUV or shipboard CTD. (bottom) Water column temperatures at the 30 m mooring location during 2011. The AUV track line or CTD station locations are shown on the top plots.

heading of 358° true for both years. All timeseries were low-pass filtered using a 40 h half power cutoff to focus on the subtidal variability.

Observations of surface wind stress, streamflow, and sea level height were obtained from NOAA and USGS databases for the study period. Winds measured by NOAA buoy 44018, located approximately 40 km northeast of the 30 m mooring, were assumed to be representative of subtidal wind variability at the moorings during 2010 and 2011. Surface winds, measured 5 m above sea level were converted to 10 m wind stresses following *Large and Pond* [1981] and assuming neutral stability. The along-shelf wind stress (Figure 3) has periods of close agreement with the near-surface Reynolds stress over much of the early portions of study periods, marked by strong variations in the along-shelf velocity. Regional sea level heights were obtained from the coastal tide gauges at stations 8418150 and 8447435 in Portland, ME and Chatham, MA, respectively (Figure 3). These data were corrected for the atmospheric pressure effect to represent the pressure anomaly present at the coast in both locations.

4. OCCC Conditions During the 2010 and 2011 Spring Transition

Hydrographic sections of temperature and salinity from 2010 and 2011 (Figures 4 and 5) illustrate both a general warming and freshening of OCCC waters between late winter and spring and summer as well as the potential for inter-annual variability in the timing and magnitude of the trends. During the earliest sampling of the current in April 2010, the coastal current was already stratified with a cold and fresh, 8°C and 30 PSU, surface plume (Figure 4). Surface waters warmed and became saltier during June and July with the hydrographic signature of the coastal current––downward sloping isopycnals––becoming most clearly
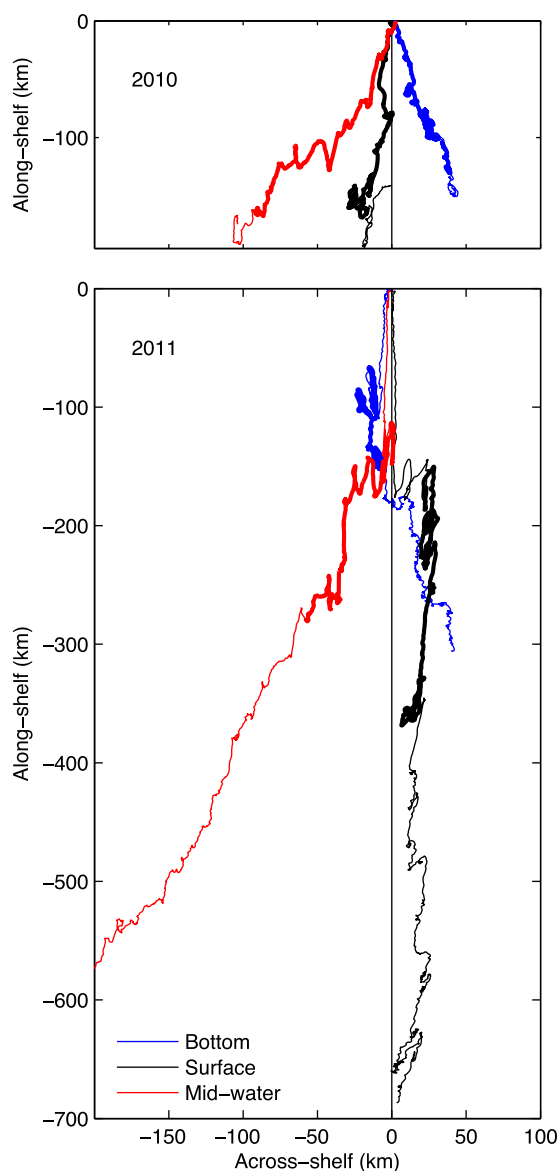
Figure 6. Progressive vector diagrams for the near-bottom (20–27 m depth), midwater (10–20 m depth), and near-surface (6–10 m depth) vector velocities from the (top) spring 2010 and (bottom) spring-summer 2011 30 m ADCP deployments. Negative along- and across-shelf distances represent southward and westward travel respectively. Thick lines on both plots represent the period of 15 April to 1 June in both years.

identified in July. In 2011 (Figure 5), water column temperatures were near 4°C and vertically uniform during March before warming to 5°C in April, and 8°C in May as lower salinity waters entered the region. Late winter salinities of 32 PSU existed onshore in the region until the beginning of May 2011, after which waters steadily freshened at the surface to 30 PSU in early June (Figure 5). By August, a stronger thermocline existed above 20 m with a separate isopycnal slope, evidence of a broad buoyant plume across the shelf with salinities as low as 29.5 PSU at the surface. Temperature stratification in 2011, a viable proxy for the total stratification at the 30 m mooring, was small until the end of April (Figure 5; bottom). While a period of weakly stratified conditions occurred in early May, the summertime stratified period did not begin in earnest until 25 May. By late summer, temperatures were up to 20°C at the surface, but as low as 7°C at depth.

The conditions in April 2011 lacked horizontal or vertical salinity gradients shoreward of the 80 m isobath, in contrast with April 2010. The temperature was well mixed in early 2011 as well, such that stratification was extremely weak in March and only slightly stratified below 40 m depth in April 2011. The conditions in spring of 2010 and 2011 are consistent with the analysis of interannual variability of the Western Maine Coastal Current presented by *Li et al.* [2014]. They noted that 2010 had the lowest salinity in April for the 2002–2011 time period. However, it is also interesting to note that minimum temperatures observed in March 2011, 3.2°C, were the lowest of the 2 year period described here, but not the lowest of the previous decade. A previous occupation of the same cross-shelf transect in March 2005 observed a minimum temperature of 2°C, the decadal minimum, which was consistent with recent documentation of anonymously cool temperatures present in the US northeast during the winter of 2004–2005 [*Forsyth et al.*, 2015].

Adding context to the hydrographic changes seen, the velocity structure measured by the 30 m ADCP illustrates the formation of the coastal current and its reversals through spring and summer. Represented using progressive vector diagrams (Figure 6), bottom waters (i.e., 20–27 m depth) flow southward and trend offshore in both years after 15 April (marked by the switch to thick lines in the figure) attaining negative southward accumulated distance and eastward across-shelf distance (Figure 6; blue line). Before this period in 2011, an initial onshore flow existed until mid-April. The middle of the water column (10–20 m depth) as well as the small portion of the near-surface water column sampled by the ADCP (6–10 m depth; representative of the surface plume present at depths above 10 m during the second half of the study period (Figure 5), also flowed generally southward, but with stronger flows closer to the surface (Figure 6). A number of large reversals of the along-shelf flow occurred within 10 days of 15 April in both years; advecting waters
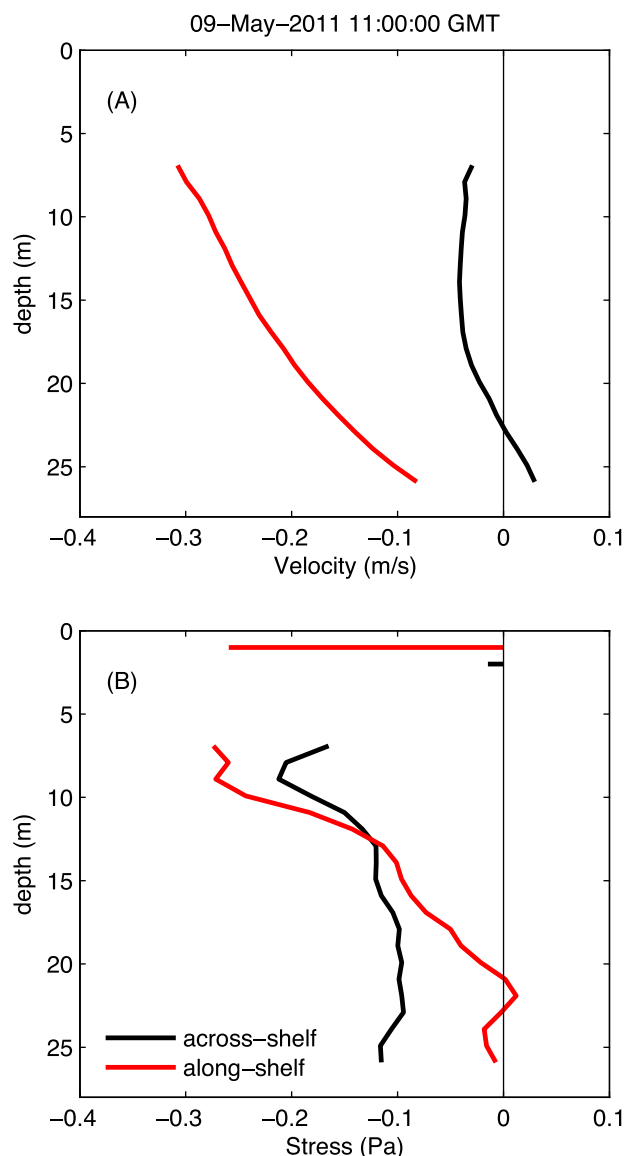
Figure 7. Example, from 9 May 2011, of the vertical structure of velocity and Reynolds stress found during times of weak stratification. (a) Along and across-shelf velocities and (b) stresses are shown with the along-shelf components shown in red. Horizontal bars near the surface in Figure 7b illustrate the direction and magnitude of the along and across-shelf wind stresses.

up to 25 km northward. These events led to the onshore/offshore split of the mid-water and near-surface waters in 2011, but only to a mild onshore surface accumulation in 2010.

Summarizing these results, the strengthening along-shelf flow during spring is interrupted by a series of flow reversals that drive a general upwelling circulation with offshore flow at the surface and onshore flow below 10 m depth. After 1 June (marked by the return to thin lines in Figure 6) the across-shelf circulation changes to a general downwelling circulation under the plume which is advected purely to the south. As summertime winds are generally weaker but predominantly northeastward and upwelling favorable during summer (Figure 3), the southward accumulation found after 1 June (Figures 3 and 6) must be due to pressure gradients or increased density forcing.

5. The Locally Relevant Pressure Gradient

5.1. Evidence of Pressure Gradient Forcing

The Reynolds stress observed at 10 m depth has periods of close agreement with the along-shelf wind stress over much of the study period (Figure 3). A representative example of the vertical structure present during these initial periods is shown by a snapshot of the subtidal velocity and stress profiles at the 30 m mooring on 9 May 2011 (Figure 7). A dominant, vertically sheared along-shelf velocity profile with secondary circulation offshore in the bottom 5 m and onshore in the remainder of the water column exists; corresponding to a vertically sheared surface-intensified along-shelf stress up to 0.3 Pa in magnitude (Figure 7). Across-shelf stresses are more uniform with depth in the bottom 20 m of the water column. This correspondence suggests that the velocity and stress dynamics are driven primarily by the along-shelf wind during much of the spring transition. However, the profile of along-shelf stress during wind forcing is uncharacteristic of simple coastal circulation forced solely by an along-shelf wind, which would be vertically uniform (i.e., no stress divergence [*Allen and Smith*, 1981; *Lentz*, 1994, 1995]), and suggests the presence of an additional body force.

Examining the role of this additional body force, the depth-averaged mean divergence of the Reynolds stresses was estimated from the slope of linear regressions to the stress profiles. The approximation of linear stress profiles was used to reduce the role of small scale structures in the divergence calculation as well as focus on the barotropic, or depth-averaged dynamics present. Comparing the estimated along-shelf stress divergence to the along-shelf wind stress (Figure 8) reveals that, in addition to the near-surface stress itself being potentially similar to the wind stress, the sign and magnitude of the stress divergence also scales
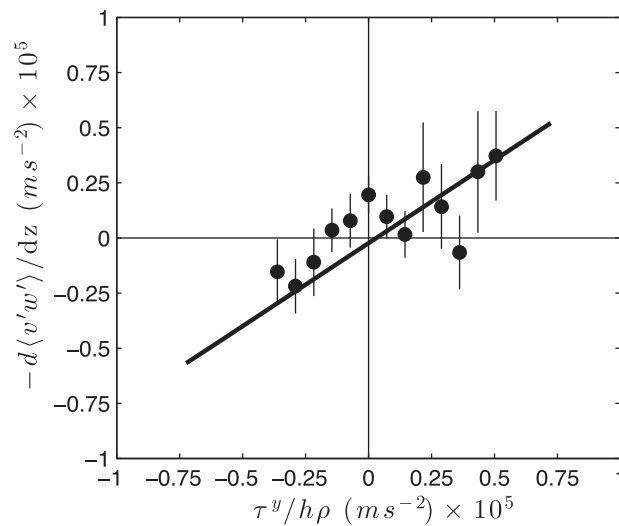
Figure 8. The vertical divergence of the along-shelf Reynolds stress versus the surface wind stress. The linear fit (thick black line: CC=0.47 with a slope of 0.77) was estimated for $|\tau^y|/h\rho < 1 \times 10^{-5}$ m s^{-2}. The correspondence between the two suggests that, in addition to the near surface Reynolds stress being correlated to the wind (Figure 3), a portion of the Reynolds stress divergence (as shown here) also appears to be related to the wind. This correlated stress divergence must be due to an unknown body force linked to the wind forcing.

with the magnitude of the wind forcing. The wind and divergence timeseries are significantly correlated (correlation coefficient CC=0.47) with a linear regression slope of 0.77. This correspondence is consistent with the existence of an along-shelf pressure gradient that is coupled with, or likely a response to, forcing from the along-shelf wind. Observed in previous studies of upwelling dynamics [*Allen and Smith*, 1981], this pressure gradient opposes the wind, creating the observed stress divergence. Using the estimated regression slope, a wind momentum input of 0.5×10^{-5} m s^{-2}, or τ^y=0.15 Pa, would coincide with an along-shelf pressure gradient of $\partial P/\partial y$=3.9 $\times 10^{-3}$ Pa/m, or a sea level gradient of $\partial\eta/\partial y$=3.8 $\times 10^{-7}$. For perspective, the mean—or background—along-shelf sea level gradient for the MAB was recently estimated to be 3.7 $\times 10^{-8}$ [*Lentz*, 2008].

While close agreement is often found between the wind and Reynolds stress estimates, they can also differ substantially, suggesting that a frictional forcing mechanism such as an along-shelf pressure gradient not driven by the wind is also present in the observed response. Thus, in addition to direct wind forcing, the frictional effects of an along-shelf pressure gradient might play a key role in the dynamics of along shelf transport and exchange along the Outer Cape. That evidence for the locally relevant pressure gradient exists in the observations of the stress dynamics also suggests that a reasonable estimate of the locally relevant pressure gradient can be made using these observations.

5.2. Estimating the Along-Shelf Pressure Gradient

Prior studies [i.e., *Lentz*, 2008] have used an inversion of the along-shelf momentum balance to estimate the locally relevant along-shelf pressure gradient. This type of inversion depends on assuming that nonlinear effects such as advective fluxes or tidal stress are small and that boundary stress parameterizations are well-tuned. Knowledge of the observed stress divergence represents a more direct way to account for the role of the boundary stresses and therefore estimate the unmeasured pressure gradient. This inverse is based on the depth-average momentum equation in the along-shelf direction, normally written as:

$$\frac{\partial \bar{v}}{\partial t} + \mathbf{\bar{u}} \cdot \nabla \bar{v} + f\bar{u} + \frac{1}{\rho_0}\frac{\partial P}{\partial y} - \frac{\tau_y^s - \tau_y^b}{\rho H} = 0, \tag{1}$$

where H is the total water depth, f is the Coriolis parameter, ρ=1025 kg m^{-3} is a reference density, $\bar{u}$ and $\bar{v}$ are the depth-averaged horizontal velocities, and P is the depth-averaged pressure anomaly. In this form, the effects of friction are included as the difference of the surface (wind) and bottom stresses (τ^s and τ^b). However, by definition

$$\frac{\tau_y^s - \tau_y^b}{\rho H} = \frac{\overline{\partial\langle v'w'\rangle}}{\partial z}, \tag{2}$$

or the difference between the boundary stress parameterizations equals the depth-averaged mean Reynolds' stress divergence.

Terms in equation (1), and their potential uncertainties were estimated as described in Appendix B. During spring, the surface wind stress, bottom stress, and velocity tendency were the dominant terms in the along-shelf momentum balance (Figure 9). Bottom stress, estimated directly from the observed stress, was weakly
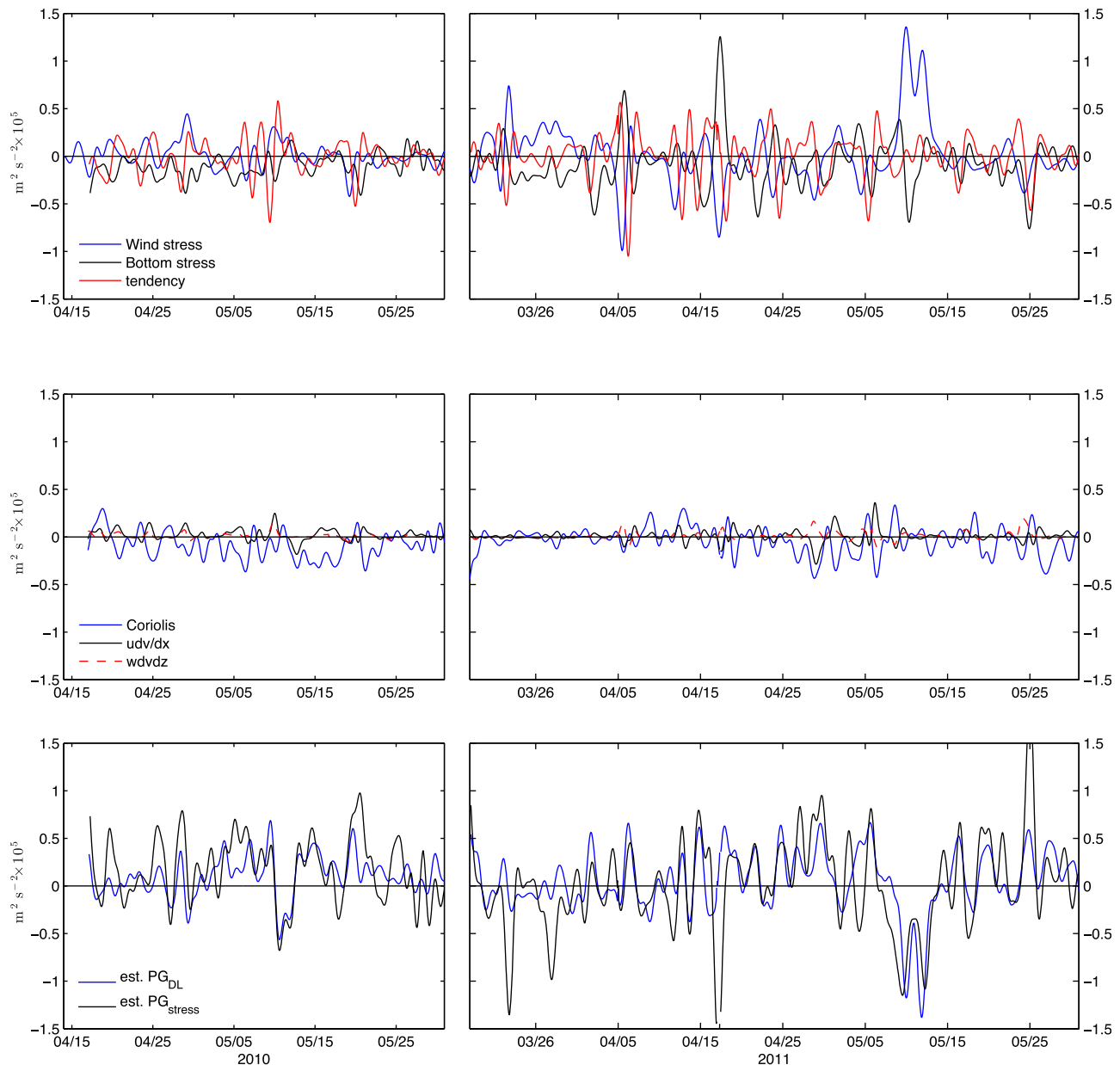
Figure 9. Observational estimates of terms in the depth-averaged along-shelf momentum balance at N30: (top) the wind stress, bottom stress, and velocity tendency (middle) the Coriolis and 2 of the 3 nonlinear advective terms, and (bottom) two estimates of the inferred along-shelf pressure gradient formed using the residual of the major terms balance and the quadratic drag law parameterization of bottom stress (PG_{DL}) and the direct estimate of the stress divergence (PG_{stress}). All terms are shown as if on the left hand side of equation (1).

negatively correlated to the wind stress in 2011 only (Table 1) and stronger than a typical parameterization based on the velocities themselves. In 2010, the correlation between the boundary stresses was not significant. Of the two, bottom stress was more often significantly correlated with the mean stress divergence. Correlations between the bottom stress and stress divergence were 0.8 and 0.57 in 2010 and 2011 respectively. Correlations between the wind stress and stress divergence were only significant in 2011, at CC=0.34 (Table 1). Importantly, the difference of the wind and bottom stresses were significantly correlated with the stress divergence, their observed equivalent, at 0.77 in 2010 and 0.81 in 2011 (Table 1). The Coriolis and nonlinear terms are generally smaller in magnitude compared to the stress and tendency terms during spring (Figure 9), although Coriolis becomes a dominant term in the balance during summer (not shown here).

These results suggest that the momentum balance during spring is dynamically simple enough, with small or uncorrelated nonlinear terms, that the stress divergence can be used to make an accurate

Table 1. Cross Correlations for Terms in the Along-Shelf Momentum Balance[a]

	$\partial v/\partial t$	$f\bar{u}$	$-\tau_s^y/\rho H$	$\tau_b^y/\rho H$	$-(\tau_s^y-\tau_b^y)/\rho H$	$\overline{\partial\langle v'w'\rangle/\partial z}$	PG_{stress}	PG_{DL}
					2010			
$\partial v/\partial t$	1.00							
$f\bar{u}$	−0.45	1.00						
$-\tau_s^y/\rho H$			1.00					
$\tau_b^y/\rho H$				1.00				
$-(\tau_s^y-\tau_b^y)/\rho H$			0.70	0.60	1.00			
$\overline{\partial\langle v'w'\rangle/\partial z}$				0.80	0.77	1.00		
PG_{stress}	−0.32			−0.67	−0.65	−0.85	1.00	
PG_{DL}	−0.58		−0.47		−0.39		0.58	1.00
					2011			
$\partial v/\partial t$	1.00							
$f\bar{u}$	−0.32	1.00						
$-\tau_s^y/\rho H$			1.00					
$\tau_b^y/\rho H$			−0.41	1.00				
$-(\tau_s^y-\tau_b^y)/\rho H$			0.67	0.40	1.00			
$\overline{\partial\langle v'w'\rangle/\partial z}$			0.35	0.57	0.81	1.00		
PG_{stress}	−0.31	−0.33		−0.50	−0.73	−0.87	1.00	
PG_{DL}	−0.44	−0.60			−0.58		0.60	1.00

[a]All terms are written as if on the left-hand side of equation (1). Only statistically significant correlations are shown.

estimate of the unknown along-shelf pressure gradient. Formed from the stress divergence, tendency, and Coriolis as:

$$PG_{stress} = -\frac{\overline{\partial\langle v'w'\rangle}}{\partial z} - \frac{\partial\bar{v}}{\partial t} - f\bar{u}, \tag{3}$$

this estimate of the time-varying along-shelf pressure gradient was significantly correlated with the difference of the boundary stresses, bottom stress, and the stress divergence itself. For context, a more typical estimate of the pressure gradient using the residuals of the boundary stress parameterizations, the velocity tendency term, and the Coriolis term as

$$PG_{DL} = -\frac{\tau_y^s-\tau_y^b}{\rho H} - \frac{\partial\bar{v}}{\partial t} - f\bar{u}, \tag{4}$$

is comparable to PG_{stress} (Table 1 and Figure 9) only after tuning the bottom stress drag coefficient to best fit the stress observations (Appendix B).

5.3. Comparing Local Versus Regional Pressure Gradients

The portion of PG_{stress} representing a response to the local wind forcing can be recreated from the wind stress timeseries by assuming a linear relationship, similar to that shown in Figure 8, exists between PG_{stress} and the wind. Using the linear regression coefficient (0.5) times the wind to estimate the wind-driven component of the pressure gradient, the estimated wind-driven pressure gradient accounts for only 22% of the variance of PG_{stress}. Thus the bulk of the estimated pressure gradient must be driven by other forcings. The nonwind driven component of the local pressure gradient places the dynamics occurring along the Outer Cape within the context of the regional Gulf of Maine dynamics [*Brown*, 1998; *Brown and Irish*, 1992].

Region-wide dynamics are perhaps best represented by the larger scale pressure gradient along the western Gulf of Maine, estimated using the difference between the coastal sea level gauges at Portland, ME and Chatham, MA. During both springs, this regional pressure gradient was uncorrelated with the local winds as well as the nonwind driven component of PG_{stress}. Additionally, there are clear time periods (e.g., 8–15 May 2010, 10–20 April 2011, 7–20 May 2011 in Figure 10) when the local pressure gradient opposes the regional gradient. Thus, the regional pressure gradient is a poor predictor of the local pressure dynamics along the Outer Cape.

6. Decomposing the Components of Along-Shelf Flow

To assess the relative importance of wind forcing on the along-shelf transport compared to the locally relevant pressure gradients and density driven geostrophic currents, the along-shelf velocity due exclusively to
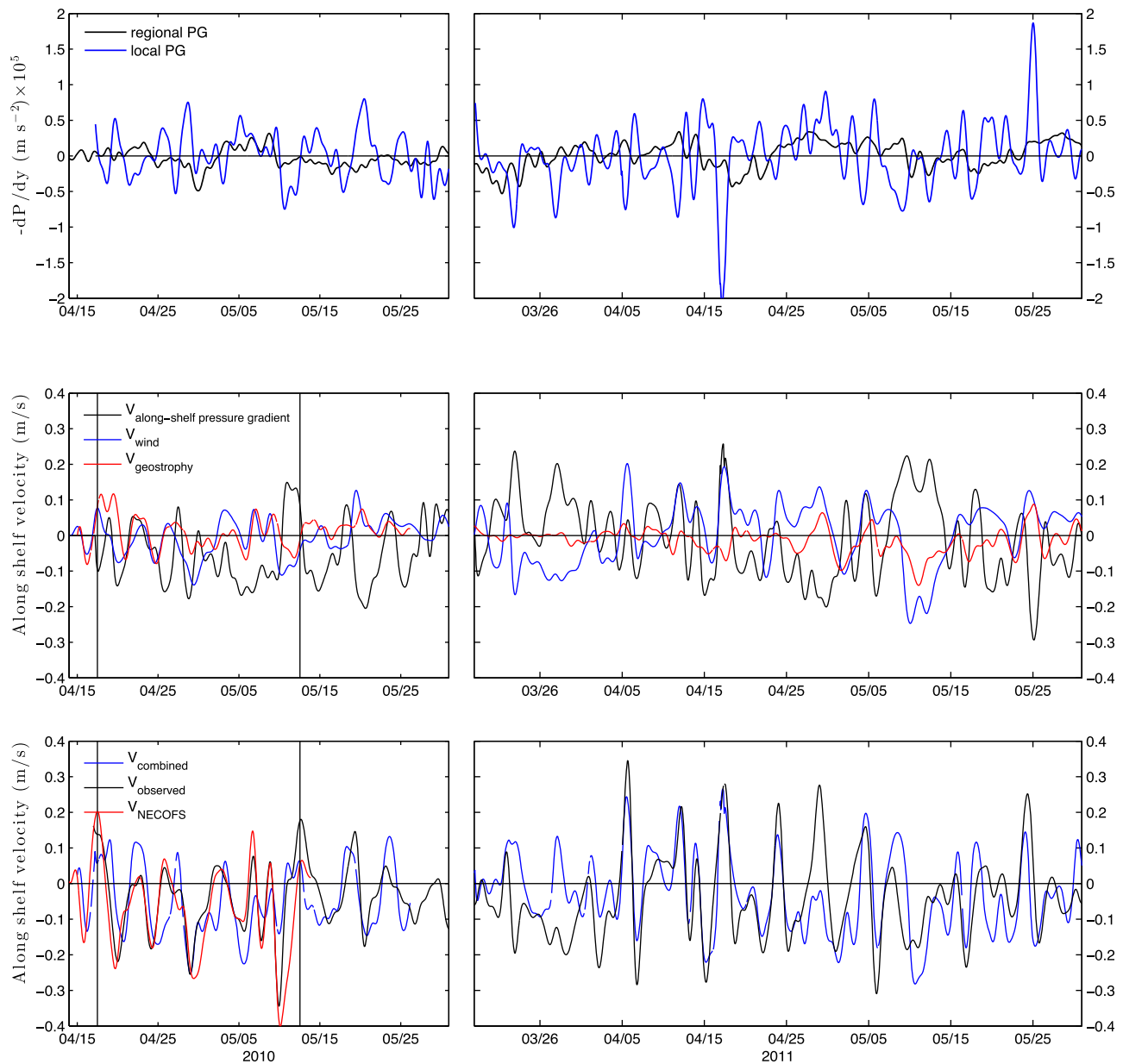
Figure 10. (top) The regional, nonwind driven pressure gradient, formed from the difference of the Portland and Chatham adjusted sea level heights, and the local nonwind driven pressure gradient for both years. (middle) Estimates of the depth-averaged along-shelf velocity due to local pressure gradient forcing, local wind forcing, and geostrophy. (bottom) The total prediction from all three components and the observed depth-averaged along-shelf velocity. For both rows, results from 2010 (2011) are shown on the left (right). The depth-averaged along-shelf velocity from the NECOFS model result nearest the study site is included for 2010, in the bottom left plot.

the observed wind or the local pressure gradient forcing were estimated using a simple one-dimensional numerical model, similar to that described by *Lentz* [1994, 1995]. The model formulation, which assumes a general structure to the eddy viscosity profile but varies its magnitude to balance the friction velocities at the boundaries, iteratively solves for the velocity structure given a known wind or along-shelf pressure gradient and the condition that $\bar{u} = 0$ to simulate the presence of a coastal boundary. A cubic parameterization for the eddy viscosity profile was chosen for use here as it is similar in structure to those found to represent inner-shelf dynamics in other locations [*Lentz*, 1994; *Lentz et al.*, 2008; *Fewings et al.*, 2008]. As the *Lentz* [1994] model essentially represents the frictional dynamics that would occur in an unstratified water column, an estimate of the portion of the observed along-shelf velocity in geostrophic balance with the across-shelf density gradient, via the thermal wind balance, was made using the depth-dependent hydrographic observations at the 30 and 60 m moorings.

The combined velocity prediction using the pressure-gradient, wind and thermal wind forcing results (Figure 10) was similar to and significantly correlated with the observed along-shelf velocity in both years (CC=0.65 in 2010 and CC=0.64 in 2011). Considering the periods before 1 June, all components examined here led to reductions of the variance of the observed along-shelf velocity (Figure 10). The density-driven along-shelf velocity accounted for 10 and 20% of the variance in 2010 and 2011 respectively. Along-shelf winds and pressure gradients had approximately equal effects on the observed along-shelf velocity, but tend to partially offset each other during key events, accounting for a combined 72–75% of the variance of the observed velocity in both years. Thus, use of the estimated pressure gradient and known winds within a simple frictional model was able to reasonably represent most of the observed along-shelf circulation. After 1 June, where pressure gradient estimates are not available, increased density-driven forcing matches the variance of a decreased wind stress and each contribute equally to the total variance, although the flow is predominately southward opposing the local wind forcing.

7. Discussion

The progression of the along-shelf velocity (section 4, Figure 6), is a proxy for the transport along the Outer Cape during the 2010 and 2011 spring transitions. Along-shelf transport during the overlapping period of 15 April to 1 June sampled in both years (Figure 6), was stronger in 2011 by 20 km of southward accumulation, representing a 10% increase. This occurred at a time of increased across-shelf flows (Figure 6) and increased vertical stratification (Figures 4 and 5) in 2010 relative to 2011. This difference in hydrography and transport was consistent with the inter-annual variability noted upstream in the Gulf of Maine by *Li et al*. [2014].

In the present study, the breakdown of the along-shelf velocity into components driven by the wind, pressure, or density forcing allows an examination of how the drivers of along-shelf transport varied between the study years. In general, local wind forcing was weaker in 2010 than in 2011, so the wind-driven along-shelf transport, was reduced as well (Figure 10), having half of the variance in 2010 relative to 2011 (0.03 versus 0.08 m^2/s^{-2}). In 2011, the geostrophically balanced velocity was generally smaller than the wind-driven or predicted pressure-driven components (Figure 10), but increased in magnitude as spring progressed. The increases in geostrophic flow seen over time in 2011 were almost exclusively southward (negative), resulting in southward net transport. In contrast, geostrophic velocity was generally larger in magnitude but variable in direction in 2010, having similar fluctuations as the wind-driven velocity throughout much of the study period. As a result, the net transport due to geostrophic flow was northward and weak in 2010.

While the inter-annual variability occurring between 2010 and 2011 [*Li et al*., 2014] had significant implications for both the local wind and density driven circulation along the Outer Cape, the inter-annual variability of the pressure-driven circulation was much smaller. The along-shelf velocity driven by the local pressure gradient was only slightly larger in variance in 2011 versus 2010 (0.008 m²/s^{-2} in 2010 and 0.01 m²/s^{-2} in 2011), and larger than the wind- and density-driven variance in both years. This suggests that the dynamical drivers of the pressure-driven circulation are independent of the gulf-wide fluctuations in freshwater input or wind forcing. Importantly, the pressure-driven velocities vary between constructively adding to the wind-driven along-shelf velocity, as seen on 17 April 2010 and 10–17 April 2011, and directly opposing the wind-driven velocities, as seen around 10 May in both years (Figure 10).

Given that pressure driven variations are large and independent of gulf-wide fluctuations on both subtidal and inter-annual timescales, the root cause of these locally relevant dynamics are of interest as they could play a potentially large role in controlling flow out of the GOM. The component of the pressure gradient correlated with the wind, likely the result of the regional wind-forced dynamics [*Allen and Smith*, 1981], would lead to pressure-driven flow that opposed the wind-driven flow. Thus when the pressure-driven velocities are either in the same direction as the wind-driven velocities or oppose and dominate the total response, the pressure-driven circulation controls exchange between the basins.

To illustrate this effect, two such periods of complementing and opposing pressure forcing are considered here in more detail. A strong northward transport event, peaking on 17 April 2010, resulted when all contributions to the local along-shelf velocity were positive or northward (Figure 10; first vertical line in the left-hand plots). In this period, the pressure-driven flow complemented the wind-driven flow, resulting in
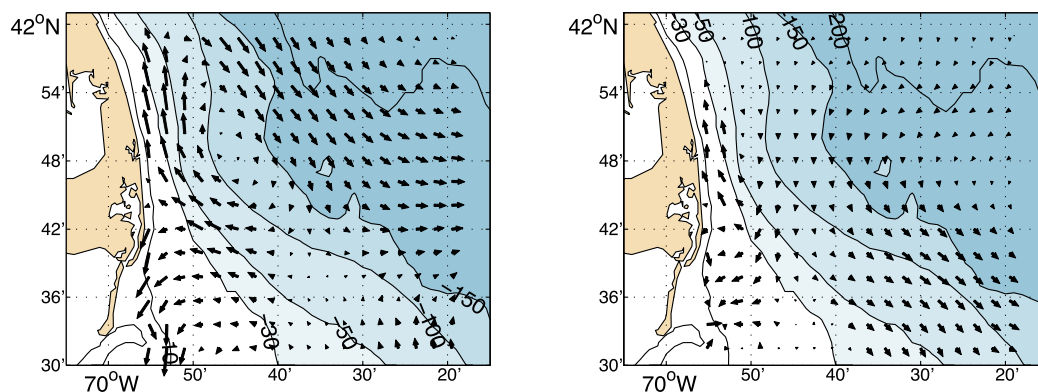
Figure 11. Depth-averaged velocities from the NECOFS hind cast simulations for two instances during 2010 in the study area when the locally relevant pressure gradient was found to oppose the regional sea level gradient: (left) 17 April, when the locally relevant pressure-driven velocities constructively added to the wind and density-driven velocities; (right) 12 May, when the locally relevant pressure-driven velocities opposed and was larger than the wind and density-driven velocities. Model output was low-pass filtered using a filter with a 40 h cut off frequency to focus on the subtidal dynamics present.

stronger along-shelf velocities. In contrast, on 12 May 2010 (Figure 10; the second vertical line) pressure-driven flow opposed and exceeded the combined magnitude of the wind-driven and geostrophic velocities, leading to a net northward along-shelf velocity when the winds and geostrophy alone would have suggested southward transport and downwelling favorable conditions.

The wider-area response of the coastal ocean during these two events were assessed using the results of the 30 year (1970–2010) hindcast model solution of circulation made using the Northeast Coastal Ocean Forecast System (NECOFS). NECOFS is an integrated atmosphere/surface wave/ocean model system configured for both hindcast and forecast applications in the northeast U.S. coastal region [*Chen et al.*, 2007, 2012]. The depth-averaged model velocity from the gridpoint nearest to the 30 m mooring location (Figure 1) for the overlapping period during 2010 (available at http://www.smast.umassd.edu:8080/thredds/dodsC/fvcom/hindcasts/30yr_gom3) was significantly correlated (CC=0.83) with the observations collected along the Outer Cape. Given this correspondence, the response of the coastal ocean present in the model is examined here to link the dynamics observed at the study location to the wider area.

On 17 April, the model depth-averaged velocity field shows northward flow near the coast at the location of the moorings, with a recirculation offshore and a divergence point to the south of the mooring location (Figure 11). This model circulation is consistent with northward winds that force a northward wind- and density-driven flow via coastal upwelling close to the coast. As a result the southward transport of the coastal current offshore is pushed offshore. The observed northward pressure driven circulation is consistent with the point of flow separation south of the mooring location at 42° N in the model (Figure 10).

On 12 May, the model depth-averaged velocity results show weaker southward flow throughout most of the domain, but strong, locally intensified northward flow near the coast. These results suggest that areas offshore are responding to the southward wind and density forcing while areas onshore are responding to the southward pressure gradient which drives flow northward. In the model, this northward flow appears to originate from the same point of flow separation seen before in 17 April, at 42° N. Velocity observations from the 60 m mooring location, available for the 2010 deployment have slightly northward flow during this time period (not shown here), indicated that the across-shelf scale of the pressure gradient may be small. While far from quantitative, analysis of the model results suggest two conclusions: the opposing along-shelf pressure gradients are generated locally along the Outer Cape, and that they act to push the along-shelf coastal current offshore long before it encounters the widening bathymetry to the south.

Finally, related to the idea of the Outer Cape as a choke point for circulation leaving the western Gulf of Maine, the local, nonwind driven along-shelf pressure gradient often opposed the regional pressure gradient observed from tide gauges (Figure 10). This opposition was most notable during April 2011. During these events, while the regional gradient is driving flow to the south and out of the Gulf of Maine, the local pressure gradient, as well as along-shelf velocities, are directed northward (Figure 10). These results suggest

that local pressure dynamics along the Outer Cape might create a "wedge" effect for the southward flowing Western Maine Coastal Current, forcing the current offshore and to the east, rather than southward along isobaths. The interaction of the pressure-gradient and wind-forced dynamics highlighted above and in the NECOFS model output illustrate the potential role of localized gradients along the Outer Cape in setting the flow conditions into the Great South Channel and Georges Bank. Although this analysis has shown that short time and space scale variabilities exist along the Outer Cape, additional observations, likely closely linked to numerical simulations, are necessary to fully understand their role on the flow leaving the Gulf of Maine, as well as setting water mass properties for inflows to Georges Bank and the Middle Atlantic Bight.

8. Summary and Conclusions

The drivers of along-shelf circulation in the southwestern portion of the Gulf of Maine and their potential variability were investigated using an innovative approach based on the observations of a single ADCP, configured to record along-beam velocities in high-frequency bursts. The resulting velocity and stress timeseries were combined with across-shelf density gradients from the moored hydrographic observations to describe all of the significant aspects of the along-shelf current. These observations on inner shelf offshore of Cape Cod, Massachusetts, defined the coastal current at a critical connection point between the Gulf of Maine at the Mid-Atlantic Bight.

The inferred circulation during the spring to summer transitional periods of 2010 and 2011 was consistent with simple models of circulation during along-shelf wind forcing, but inclusion of an along-shelf pressure gradient that scaled with the wind stress was required to match observations during times of along-shelf wind forcing. Inferring the barotropic along-shelf pressure gradients present from the momentum balance revealed a sizable component that was not driven by the along-shelf winds and often opposed the regional pressure gradient. Using a simple model to recreate the components of the along-shelf velocity, local along-shelf winds and pressure gradients dominate the along-shelf circulation during the spring transition, often with opposing forcing that can arrest the along-shelf flow over the inner shelf. Interpreted in the light of complex, regional numerical simulations, the observations here suggest an offshore divergence of the main along-shelf current exiting the Gulf of Maine during spring and illustrate that local dynamics along the Outer Cape might have broad implications for the exchange between the Gulf of Maine and the Mid-Atlantic Bight.

Appendix A: Estimating Reynolds Stresses

Estimates of the vertical Reynolds stresses were obtained following the cospectra-fit (CF) method [*Kirincich et al.*, 2010]. The CF method fits a model of the turbulent velocity cospectrum [*Kaimal et al.*, 1972] to the observed cospectrum at wavenumbers greater than those of surface gravity waves to estimate the total covariance (the Reynolds stress) and the "roll-off" wavenumber (k_o), a measure of the dominant length scale of turbulent fluctuations. An inherent benefit of using this model fit approach is its ability to correct for biases of the estimated stresses due to the ADCP's large bin-size [i.e., *Stacey et al.*, 1999b], as long as the dominant eddy size is captured within the below-waveband cospectra. For the data set analyzed here, a maximum frequency of 1/8 Hz was used for the waveband cutoff frequency. Following *Kirincich et al.* [2010], successful stress estimates were available 60% of the time during weakly-stratified conditions and less frequently during more stratified conditions. Instrument noise was a significant issue for individual stress estimates, as the ADCP observations were collected using the standard water track ping mode (mode-1).

To focus on the subtidal scales of variability present in the stress results and to reduce the effects of noise, hourly-averaged observations from only those times and depths with viable stress estimates were interpolated using a spline-fit to fill in gaps between the top and bottom available observations and reduce the effect of noise on each individual profile [e.g., *Stacey et al.*, 1999a]. A spline smoothing factor of 0.8 was found, by inspection, to eliminate obvious spikes while preserving the overall shape of the profile. Additional near-bottom or near-surface gaps in the stress profiles shorter than 10 h were linearly interpolated before low-pass filtering in time using a filter with a 40 h half-power cutoff. Error estimates ranged from 1 to 2×10^{-4} m^2 s^{-2} for raw stress estimates, but decrease to less than 0.5×10^{-4} m^2 s^{-2} for the hourly averaged, vertically splined, and temporally filtered data product used here. To avoid the increases in stress errors due to the effects of increased stratification [*Stacey et al.*, 1999b; *Kirincich*, 2013], as well as to focus

on times when the role of the stresses on momentum transfer through the water column might be more simplified, analysis of the stress dynamics is restricted to the deployment periods before 1 June each year, when the water column at 30 m depth was usually weakly stratified (Figures 4 and 5).

Appendix B: Estimating Terms in the Along-Shelf Momentum Balance

The magnitude of the wind stress, Coriolis, tendency, and two of the three advective terms in equation (1), the across-shelf flux of along-shelf momentum ($u\partial v/\partial x$) and the vertical flux of along-shelf momentum ($w\partial v/\partial z$), were estimated following *Lentz et al.* [1999] using the velocity profiles measured by the ADCP before depth-averaging. While the surface wind stress was estimated from buoy wind observations using bulk formula, as described above, a more direct estimate of the bottom stress term was made utilizing the along-shelf Reynolds stress at the bottom-most bin of the ADCP. This estimate was correlated (CC=0.74) with a quadratic parameterization of bottom stress using the horizontal velocities from the bottom-most bin (at a height of 3 m). A linear regression between the two for 2011 suggested a drag coefficient (C_D) of 4.3×10^{-3}. This is notably higher than the 1.5×10^{-3} typically assumed for these types of open shelf conditions and heights above the bottom [*Lentz*, 2008]. Rough estimates of $u\partial v/\partial x$ and $w\partial v/\partial z$ were made based on the following assumptions: (1) $\bar{u}=0$ and $v=0$ at the coast, and (2) w has a parabolic structure with a maximum value that balances observed across-shelf transport. The third nonlinear term, the along-shelf flux of along-shelf momentum could not be estimated with the data at hand, however scaling analysis suggests it is likely the same or less than the other nonlinear terms. Uncertainties for all terms were estimated following *Lentz et al.* [1999]. Burst-averaged and/or depth-averaged velocities generally have uncertainties of 1×10^{-2} m s^{-1}, making the uncertainty of the Coriolis term the largest of those estimated (1×10^{-6} m s^{-2}), not including the errors related to the assumptions used to estimate the nonlinear terms.

References

Allen, J. (1980), Models of wind-driven currents on the continental shelf, *Annu. Rev. Fluid Mech.*, *12*, 389–433.

Allen, J. A., and R. Smith (1981), On the dynamics of wind-driven shelf currents, *Philos. Trans. R. Soc. London A*, *302*, 617–634.

Anderson, D. M., et al. (2014), Alexandrium fundyense cysts in the Gulf of Maine: Long-term time series of abundance and distribution, and linkages to past and future blooms, *Deep. Sea Res., Part II*, *103*, 6–26, doi:10.1016/j.dsr2.2013.10.002.

Balch, W., D. Drapeau, B. Bowler, and T. Huntington (2012), Step-changes in the physical, chemical and biological characteristics of the Gulf of Maine, as documented by the GNATS time series, *Mar. Ecol. Prog. Ser.*, *450*, 11–35, doi:10.3354/meps09555.

Beardsley, R. C., P. C. Smith, and C. M. Lee (2003), Introduction to special section: U.S. GLOBEC: Physical processes on Georges Bank, *J. Geophys. Res.*, *108*(C11), 8000, doi:10.1029/2003JC002165.

Bigelow, H. B. (1927), Physical oceanography of the Gulf of Maine, *Fish. Bull.*, *40*, 511–1027.

Bothner, M. H., and B. E. Butman (2007), Processes influencing the transport and fate of contaminated sediments in the coastal ocean-Boston Harbor and Massachusetts Bay, *U.S. Geol. Surv. Circ. 1302*, 89 p.

Brink, K. H., R. Limeburner, and R. C. Beardsley (2003), Properties of flow and pressure over Georges Bank as observed with near-surface drifters, *J. Geophys. Res.*, *108*(C11), 8001, doi:10.1029/2001JC001019.

Brown, W. (1998), Wind-forced pressure response in the Gulf of Maine, *J. Geophys. Res.*, *103*, 30,661–30,678.

Brown, W., and J. Irish (1992), The annual evolution of geostrophic flow in the Gulf of Maine: 1986-1987, *J. Phys. Oceanogr.*, *22*, 445–473.

Chen, C., R. C. Beardsley, and R. Limeburner (1995a), Variability of currents in late spring in the northern Great South Channel, *Cont. Shelf Res.*, *15*, 451–473.

Chen, C., R. C. Beardsley, and R. Limeburner (1995b), Variability of water properties in late spring in the northern Great South Channel, *Cont. Shelf Res.*, *15*, 415–431.

Chen, C., H. Huang, R. C. Beardsley, H. Liu, and G. W. Cowles (2007), A finite-volume numerical approach for coastal ocean circulation studies: Comparisons with finite difference models, *J. Geophys. Res.*, *112*, C03018, doi:10.1029/2006JC003485.

Chen, C., et al. (2012), An unstructured-grid, finite-volume community ocean model FVCOM user manual (3rd edition), *Tech. Rep. 11-1101*, School of Marine Science and Technology/University of Massachusetts at Dartmouth (SMAST/UMASSD).

Churchill, J. H., N. R. Pettigrew, and R. P. Signell (2005), Structure and variability of the western Maine coastal current, *Deep. Sea Res., Part II*, *52*, 2392–2410, doi:10.1016/j.dsr2.2005.06.019.

Durbin, E. G., A. G. Durbin, and R. C. Beardsley (1995), Springtime nutrient and chlorophyll a concentrations in the southwestern Gulf of Maine, *Cont. Shelf Res.*, *15*, 433–450.

Fewings, M., S. J. Lentz, and J. Fredericks (2008), Observations of cross-shelf flow driven by cross-shelf winds on the inner continental shelf, *J. Phys. Oceanogr.*, *38*, 2358–2378.

Fong, D., W. Geyer, and R. Signell (1997), The wind-forced response on a buoyant coastal current: Observations of the western Gulf of Maine plume, *J. Mar. Syst.*, *12*(1-4), 69–81, doi:10.1016/S0924-7963(96)00089-9.

Forsyth, J., M. Andres, and G. Gawarkiewicz (2015), Recent accelerated warming of the continental shelf off New Jersey: Observations from the CMV Oleander expendable bathythermograph line, *J. Geophys. Res. Oceans*, *120*, 2370–2384, doi:10.1002/2014JC010516.

Geyer, W. R., P. S. Hill, and G. C. Kineke (2004), The transport, transformation and dispersal of sediment by buoyant coastal flows, *Cont. Shelf Res.*, *24*(7), 927–949.

He, R., D. J. McGillicuddy, D. R. Lynch, K. W. Smith, C. A. Stock, and J. P. Manning (2005), Data assimilative hindcast of the Gulf of Maine coastal circulation, *J. Geophys. Res.*, *110*, C10011, doi:10.1029/2004JC002807.

He, R., D. J. McGillicuddy, D. Anderson, and B. Keafer (2008), Gulf of Maine circulation and harmful algal bloom in summer 2005: Part 1: In-situ observation of coastal hydrography and circulation, *J. Geophys. Res.*, *113*, C07039, doi:10.1029/2007JC004691.

Kaimal, J., J. C. Wyngaard, Y. Izumi, and O. R. Cote (1972), Spectral characteristics of surface-layer turbulence, *Q. J. R. Meteorol. Soc.*, *98*, 389–563.

Kirincich, A. R. (2013), Long-term observations of turbulent Reynolds stresses over the inner continental shelf, *J. Phys. Oceanogr.*, *43*(12), 2752–2771, doi:10.1175/JPO-D-12-0153.1.

Kirincich, A. R., and J. H. Rosman (2010), A comparison of methods for estimating stresses from ADCP measurements in wavy environments, *J. Atmos. Oceanic Technol.*, *28*, 1539–1553.

Kirincich, A. R., S. J. Lentz, and G. P. Gerbi (2010), Calculating Reynolds stresses from ADCP measurements in the presence of surface gravity waves using the cospectra fit method, *J. Atmos. Oceanic Technol.*, *27*, 889–907.

Large, W. G., and S. Pond (1981), Open ocean momentum flux measurements in moderate to strong winds, *J. Phys. Oceanogr.*, *11*, 324–336.

Lentz, S. J. (1994), lentz_NCal_ISdyn_JPO_1994.pdf, *J. Phys. Oceanogr.*, *24*, 2461–2478.

Lentz, S. J. (1995), Sensitivity of the inner-shelf circulation to the form of the eddy viscosity profile, *J. Phys. Oceanogr.*, *25*, 19–28.

Lentz, S. J. (2008), Observations and a model of the mean circulation over the Middle Atlantic Bight Continental Shelf, *J. Phys. Oceanogr.*, *38*(6), 1203–1221, doi:10.1175/2007JPO3768.1.

Lentz, S. J., R. T. Guza, S. Elgar, F. Feddersen, and T. H. C. Herbers (1999), Momentum balances on the North Carolina inner shelf, *J. Geophys. Res.*, *104*, 18,205–18,226.

Lentz, S. J., M. Fewings, P. Howd, J. Fredericks, and K. Hathaway (2008), Observations and a model of undertow over the inner continental shelf, *J. Phys. Oceanogr.*, *38*, 2341–2357.

Li, Y., R. He, and D. J. McGillicuddy (2014), Seasonal and interannual variability in Gulf of Maine hydrodynamics: 2002-2011, *Deep Sea Res., Part II*, *103*, 210–222, doi:10.1016/j.dsr2.2013.03.001.

Manning, J., D. McGillicuddy, N. Pettigrew, J. Churchill, and L. Incze (2009), Drifter observations of the Gulf of Maine coastal current, *Cont. Shelf Res.*, *29*(7), 835–845, doi:10.1016/j.csr.2008.12.008.

McGillicuddy, D., C. A. Signell R.P. Stock, B. A. Keafer, M. D. Keller, R. D. Hetland, and D. M. Anderson (2003), A mechanism for offshore initiation of harmful algal blooms in the coastal Gulf of Maine, *J. Plankton. Res.*, *5*(9), 1131–1138.

McGillicuddy, D. J., D. W. Townsend, B. A. Keafer, M. A. Thomas, and D. M. Anderson (2014), Georges Bank: A leaky incubator of Alexandrium fundyense blooms, *Deep Sea Res., Part II*, *103*, 163–173, doi:10.1016/j.dsr2.2012.11.002.

Pettigrew, N., J. H. Churchill, C. D. Janzen, L. J. Mangum, R. P. Signell, A. C. Thomas, D. W. Townsend, J. P. Wallinga, and H. Xue (2005), The kinematic and hydrographic structure of the Gulf of Maine Coastal Current, *Deep Sea Res., Part II*, *52*, 2369–2391.

Pringle, J. M., A. M. H. Blakslee, J. E. Byers, and J. Roman (2011), Asymmetric dispersal allows an upstream region to control population structure throughout a species' range, *Proc. Natl. Acad. Sci. U. S. A.*, *108*(37), 15,288–15,293.

Rosman, J. H., J. L. Hench, J. R. Koseff, and S. G. Monismith (2008), Extracting Reynolds stresses from acoustic Doppler current profiler measurements in wave-dominated environments, *J. Atmos. Oceanic Technol.*, *25*(2), 286–306, doi:10.1175/2007JTECHO525.1.

Shcherbina, A. Y., and G. G. Gawarkiewicz (2008a), A coastal current in winter: Autonomous underwater vehicle observations of the coastal current east of Cape Cod, *J. Geophys. Res.*, *113*, C07030, doi:10.1029/2007JC004306.

Shcherbina, A. Y., and G. G. Gawarkiewicz (2008b), A coastal current in winter: 2. Wind forcing and cooling of a coastal current east of Cape Cod, *J. Geophys. Res.*, *113*, C10014, doi:10.1029/2008JC004750.

Stacey, M. T., S. G. Monismith, and J. R. Burau (1999a), Measurements of Reynolds stress profiles in unstratified tidal flow, *J. Geophys. Res.*, *104*, 10,933–10,949.

Stacey, M. T., S. G. Monismith, and J. R. Burau (1999b), Observations of turbulence in a partially stratified estuary, *J. Phys. Oceanogr.*, *29*, 1950–1970.